

# 1 paper de la onda 3

*Elio Campitelli*

*April 19, 2018*

## “Tradicional” analysis.

Now this has some problems... yada yada yada, alternative analysis.

## New seasons

This text is no longer valid:

PC1 to PC4 represent the principal modes of variability of the geopotential field with wavenumber greater than 1...

PC1 and PC2 both are dominated by a wave 3 pattern. They both explain an almost equal proportion of the total variance and represent a wave 3 pattern offset by 1/4 wavelength. From that, one can infer that they are degenerated modes that represent the same wave pattern and it's meridional movement. PC3 is mainly a hemispheric scale wave 2 with a small contribution of wave 4 north of 45°S. PC4 exhibits a more complex pattern with both waves 2 and 3 contributing to the field. The result is a wave 3-ish pattern on the eastern hemisphere that affects the Atlantic and the Indian oceans but disappears over the central-south Pacific.

This result suggest that the ZW3 could be represented by a linear combination of PC1 and PC2 at the same time preserving it's meridional propagation and zonal variation.

An optimal (if somewhat arbitrary) division of the year can be seen in Figure X based on monthly mean values of each PC...

Notes:

- Making other (still sensible) decisions lead to some differences in clustering. For example, using fields with QS1 *and* QS2 filtered out puts May closer to April, and December further from JFM. Not surprisingly, a similar result is achieved by using idealized fields from the reconstructed zonal wave 3 (since higher wavenumbers explain a negligible proportion of the variance). JFM and ASO (and its similarity with April), on the other hand, are robust trimesters.
- These differences imply that the ZW2 might be have an important role in the variability in May and December.
- JJ is a relatively robust grouping but with obviously more heterogeneous than JFM or ASO
- Furthermore, removing the linear trend as well as the QS1 field results in a similar classification to the one shown, but the structure of the EOF is slightly different with less separation between wavenumbers (the zonal wave 3 is present in PC1, PC2 and PC3) and a much more asymmetric nature, with higher amplitude anomalies on the western hemisphere than the eastern in the first two PCs and the reverse on the second two. Is it as the wave activity of each hemisphere is separated this way.

## Regressions

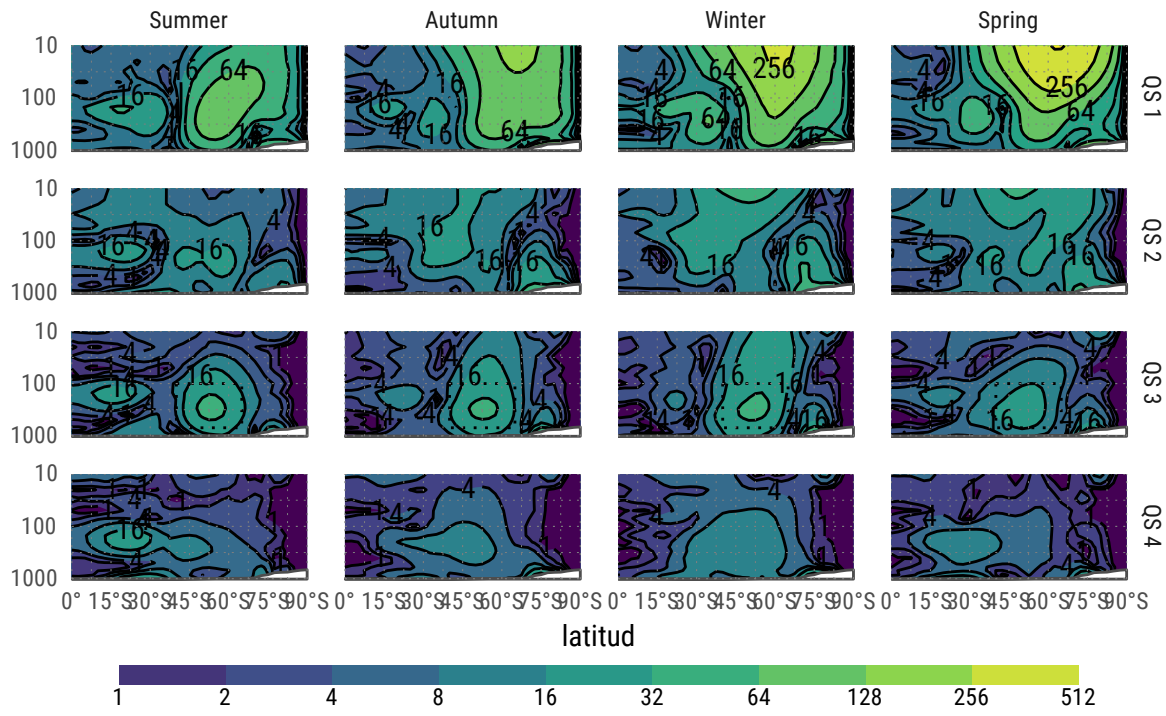


Figure 1: Fourier amplitude of geopotential height

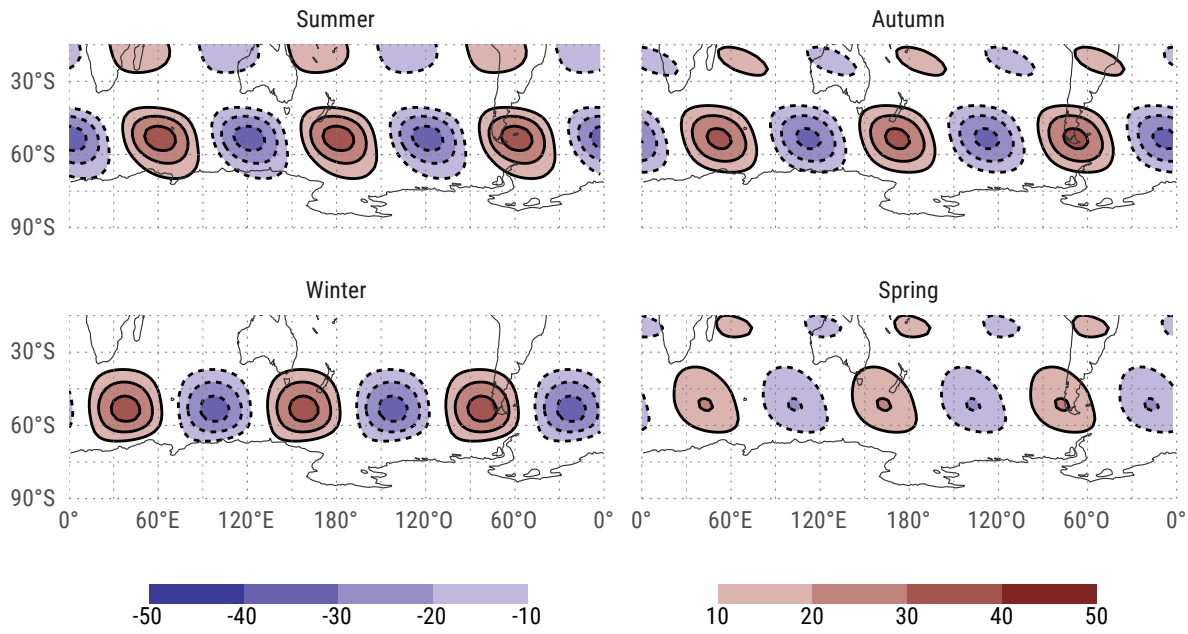


Figure 2: Wave 3 component of the geopotential field of each season at 200hPa.

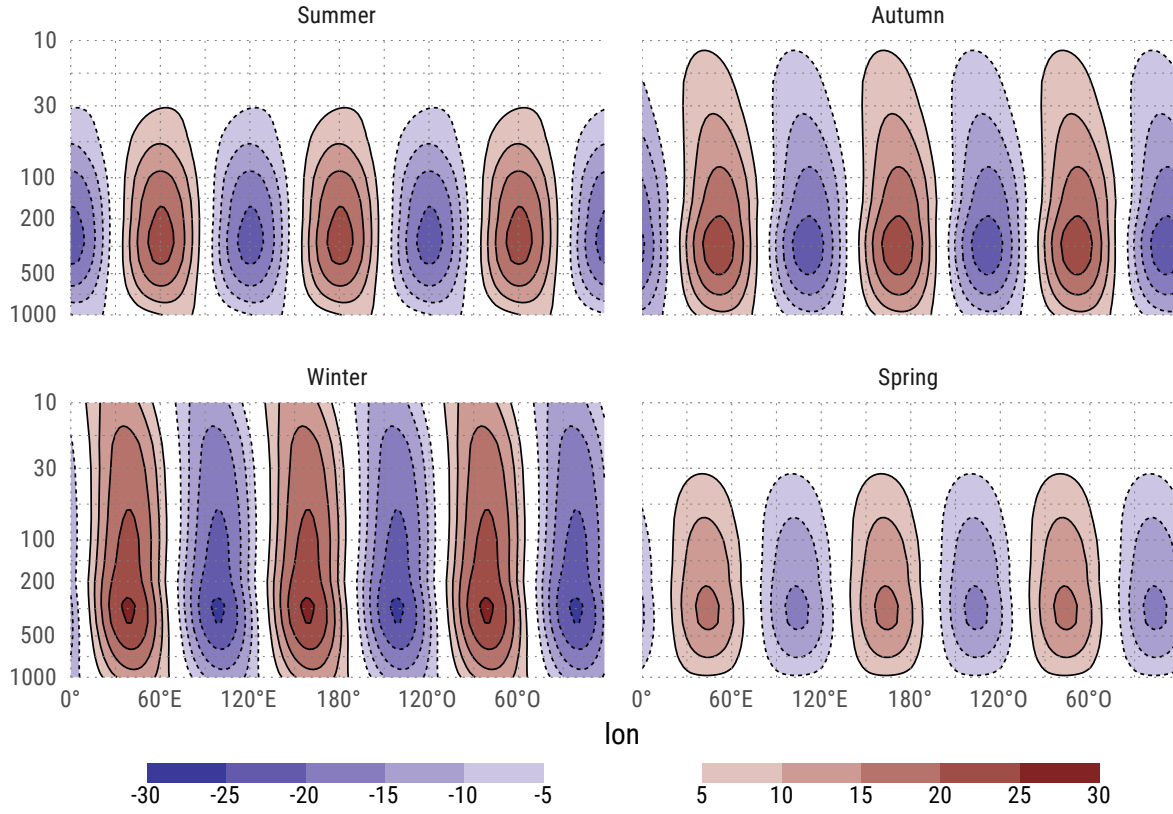


Figure 3: Mean wave 3 component of geopotential height between 65°S and 35°S

Table 1: Correlation between ONI and PC1

season	estimate_PC1	p.value_PC1
JFM	0.46	0.009623576
MJJ	0.37	0.040274550
ASO	0.36	0.045109843
ND	0.38	0.037424360

## QS3

The first two principal modes are closely related to the zonal wave 3. In fact, it can be shown that they define a rotation of the complex plane defined by the real and imaginary part of the wave3 fourier transform.

PC	PC1	PC2
R	0.0233449	-0.0225729
I	-0.0263299	-0.0250784

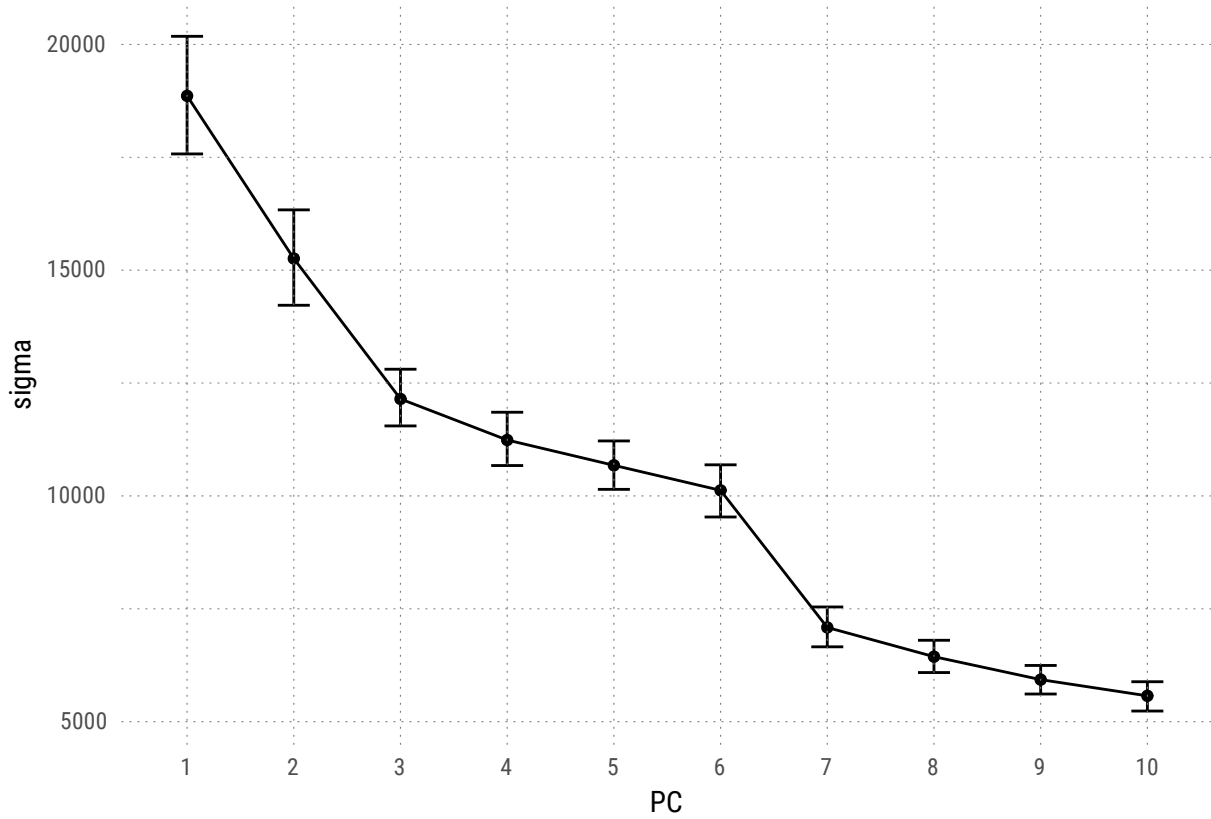


Figure 4: First 4 EOFs derived from the 200hPa detrended geopotential zonal anomaly field between 30°S and 80°S with zonal wave 1 filtered out. Errors bars represent the 95% quantile range estimated via bootstrap.

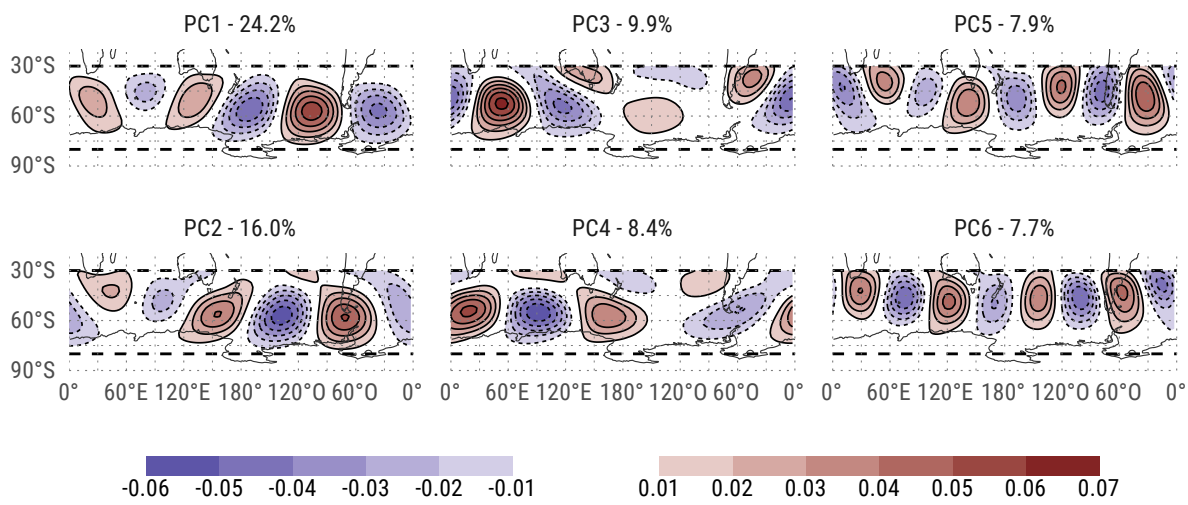


Figure 5: EOFs

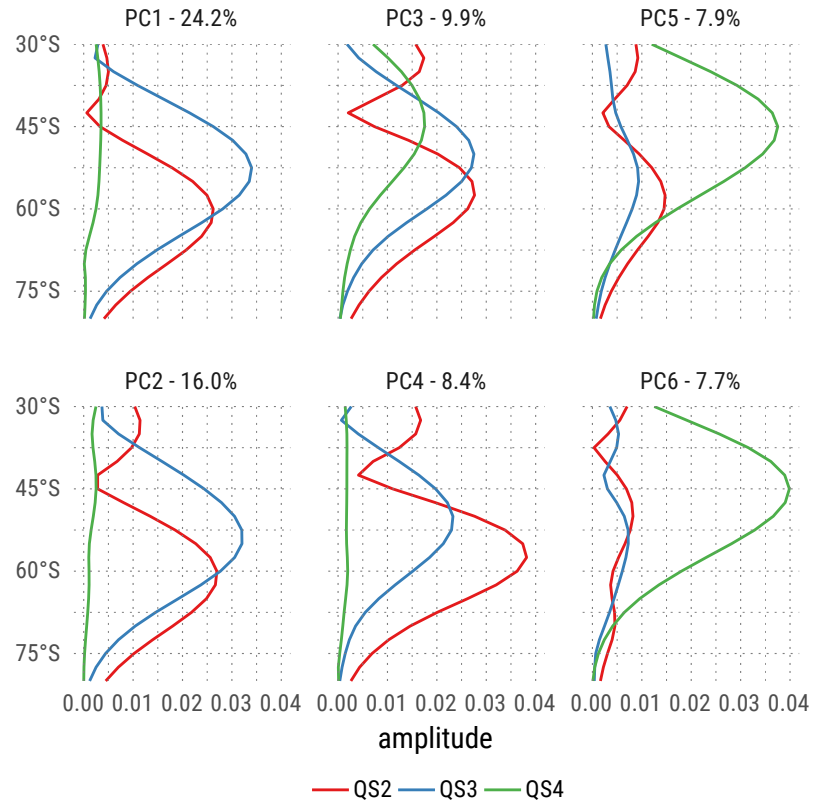


Figure 6: Fourier decomposition by latitude of each EOF.

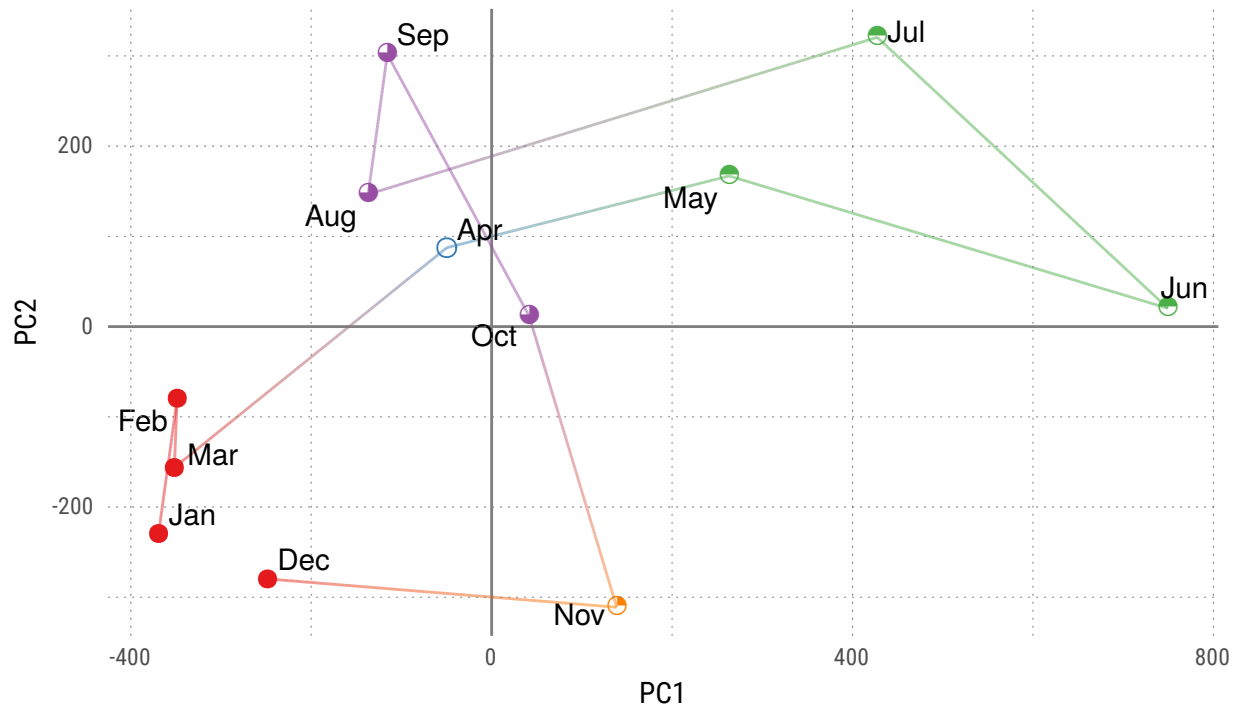


Figure 7: Monthly mean values for each PC. Colors and shapes divide months into 5 ‘seasons’.

## Cluster Dendrogram

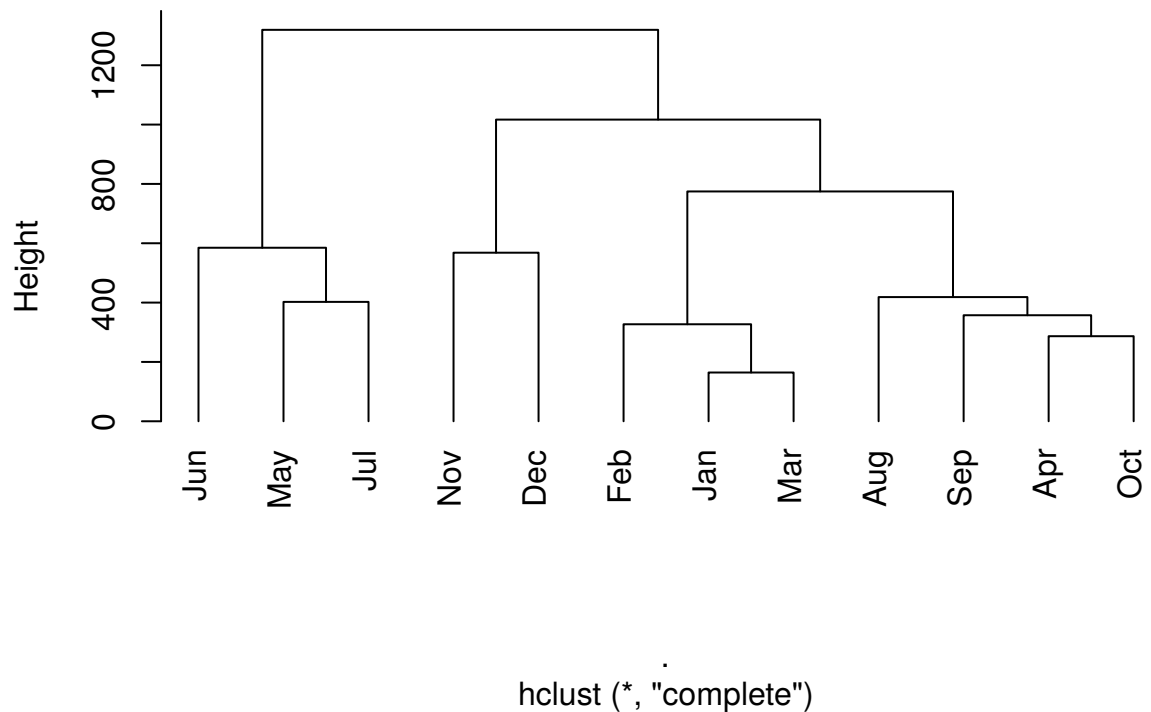


Figure 8: Hierarchical clustering of the months of the year according to the mean value of each PC scaled by it's variance.

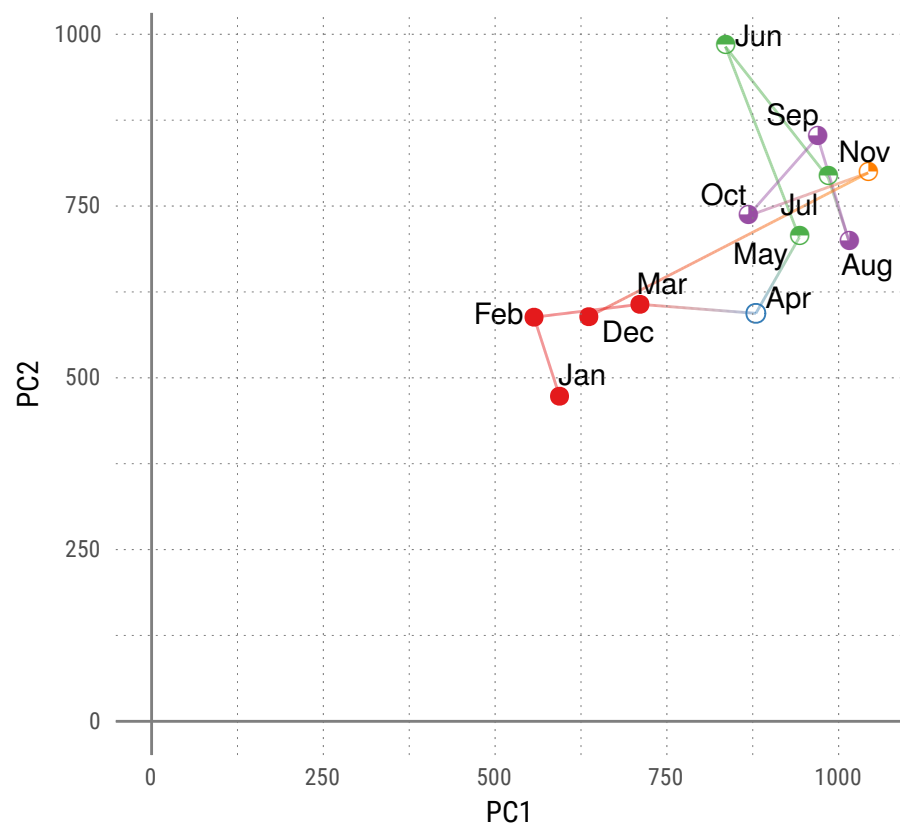


Figure 9: Monthly standard deviation for each PC. Colors and shapes divide months into 5 ‘seasons’.

## Cluster Dendrogram

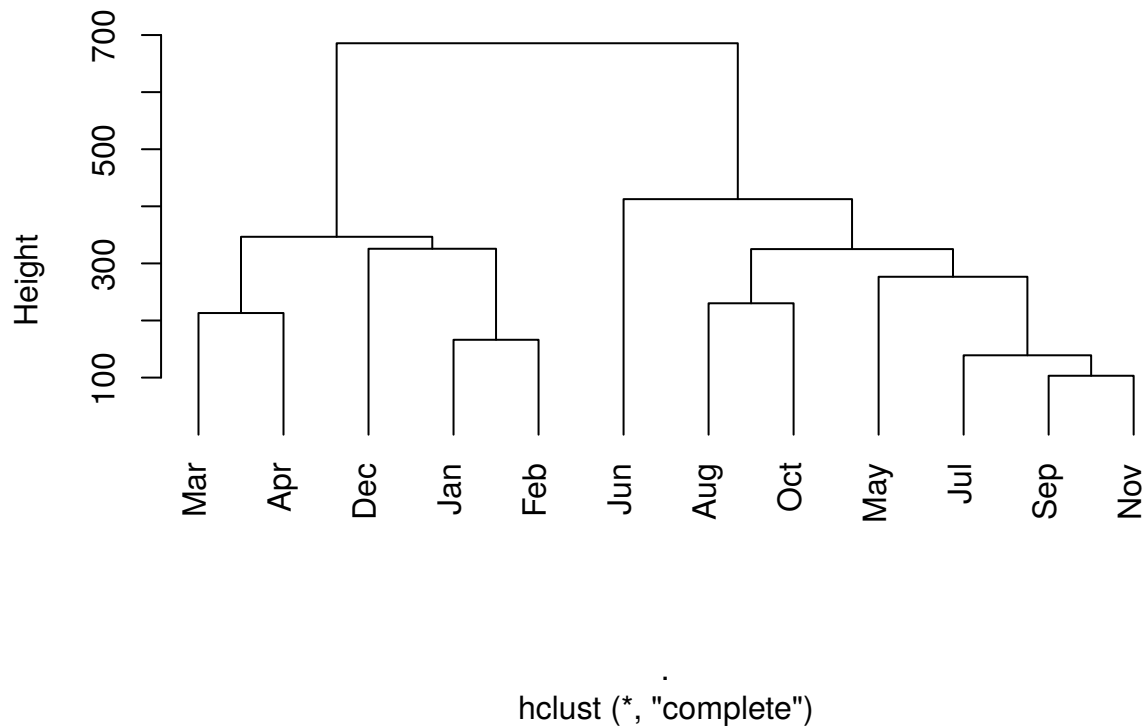


Figure 10: Hierarchical clustering of the months of the year according to the standard deviation of each PC scaled by it's variance.

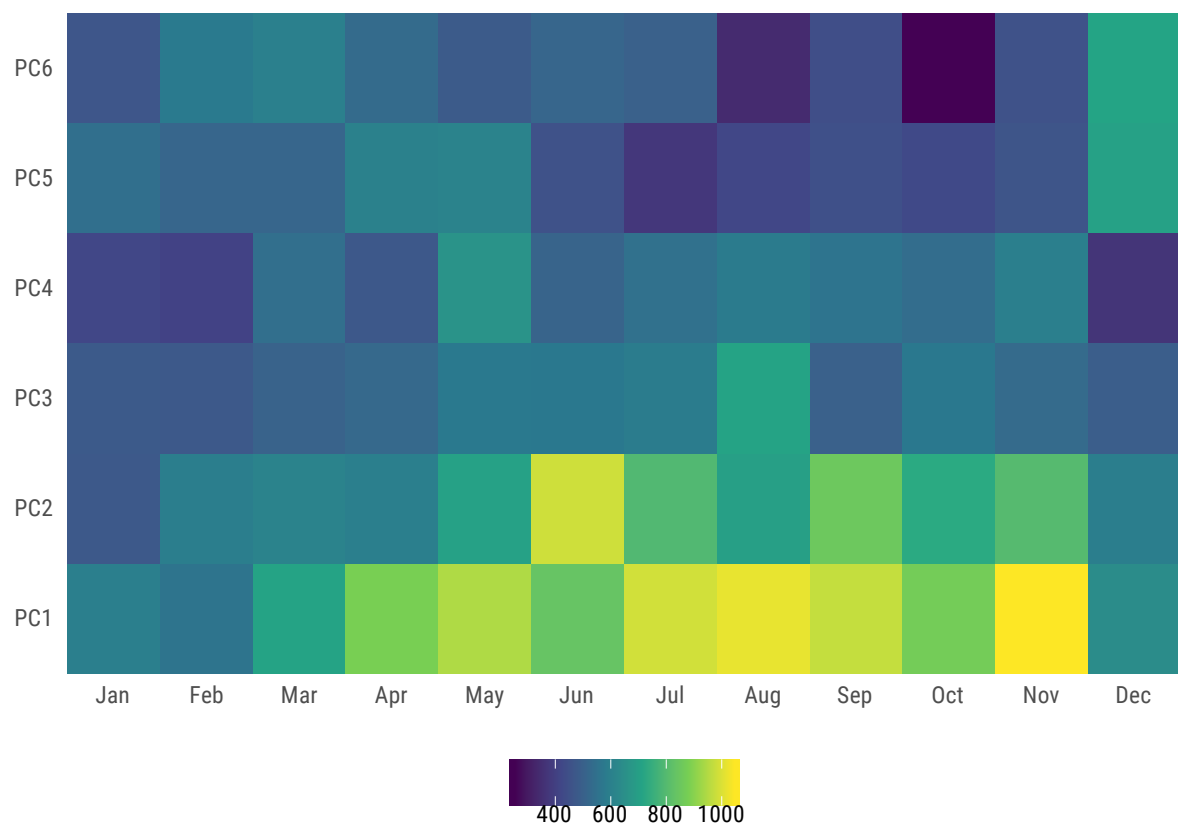


Figure 11: Standard deviation (scaled by their variance) of each PC for each month

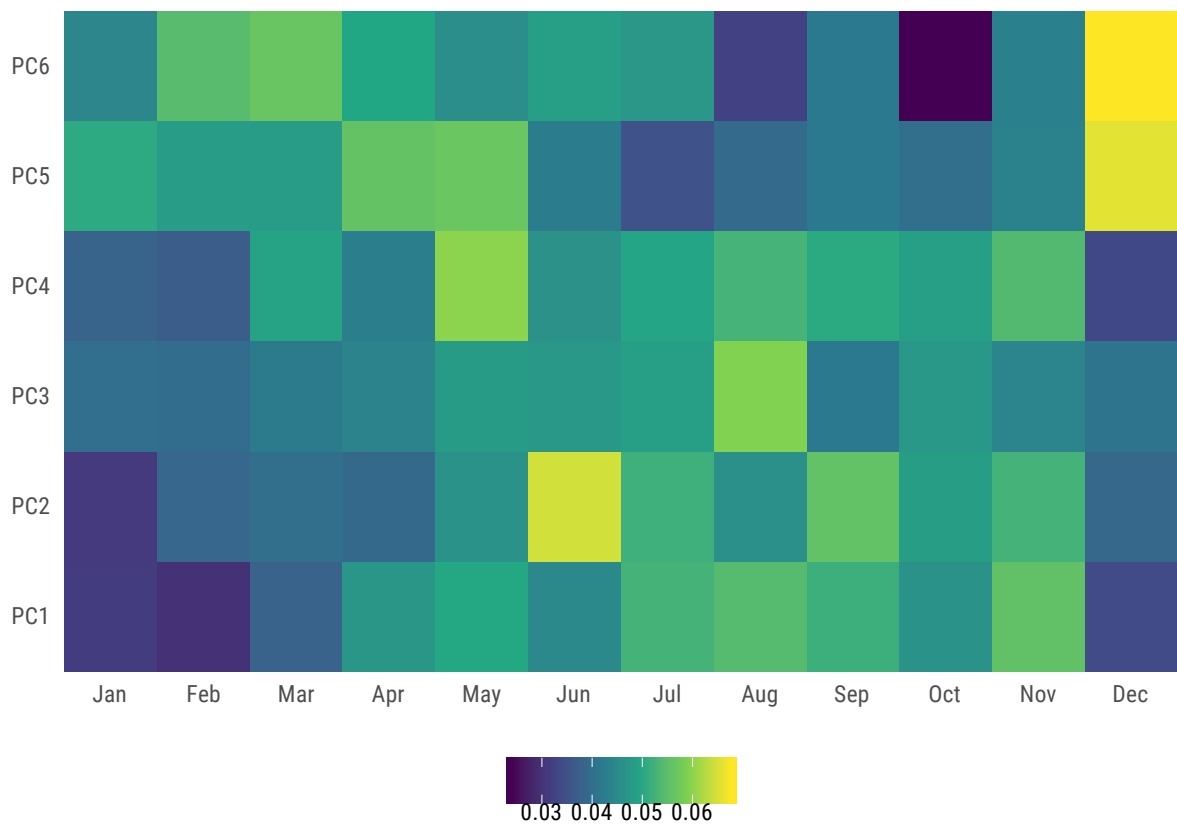


Figure 12: Standard deviation of each PC for each month

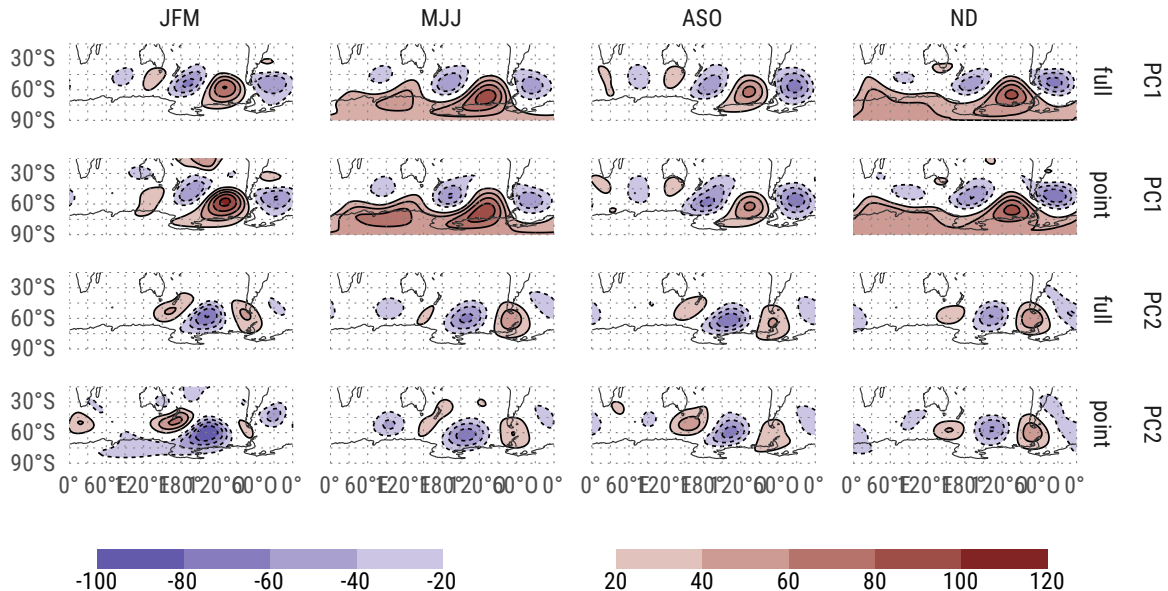


Figure 13: (standardized) Regression between PCs and ghi.

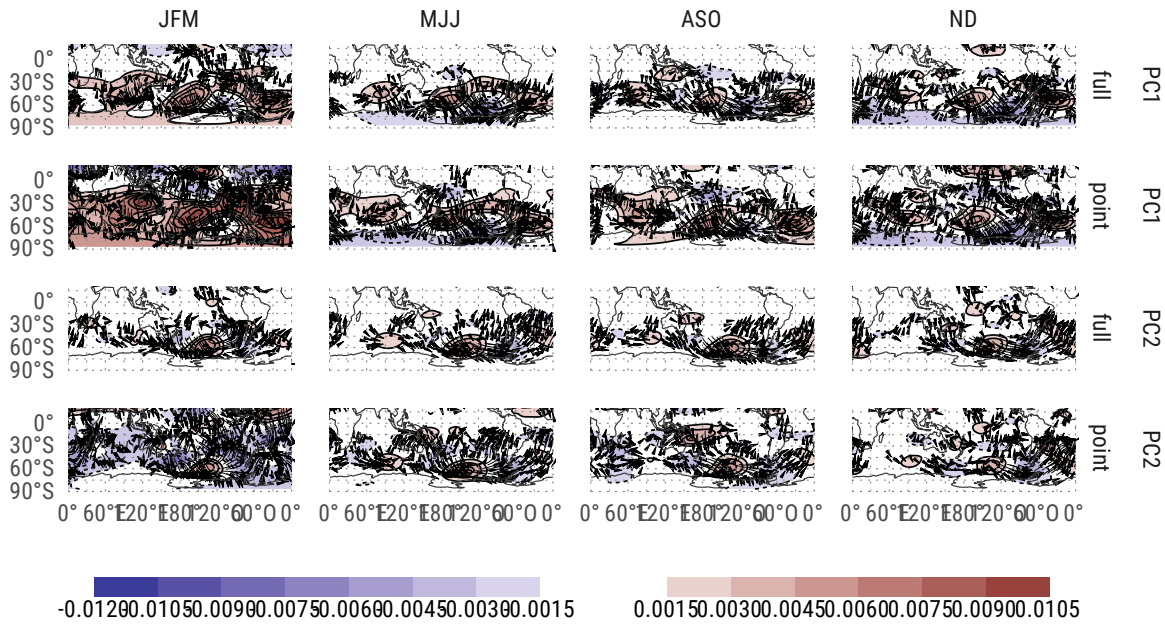


Figure 14: Regression between PCs and Psi.

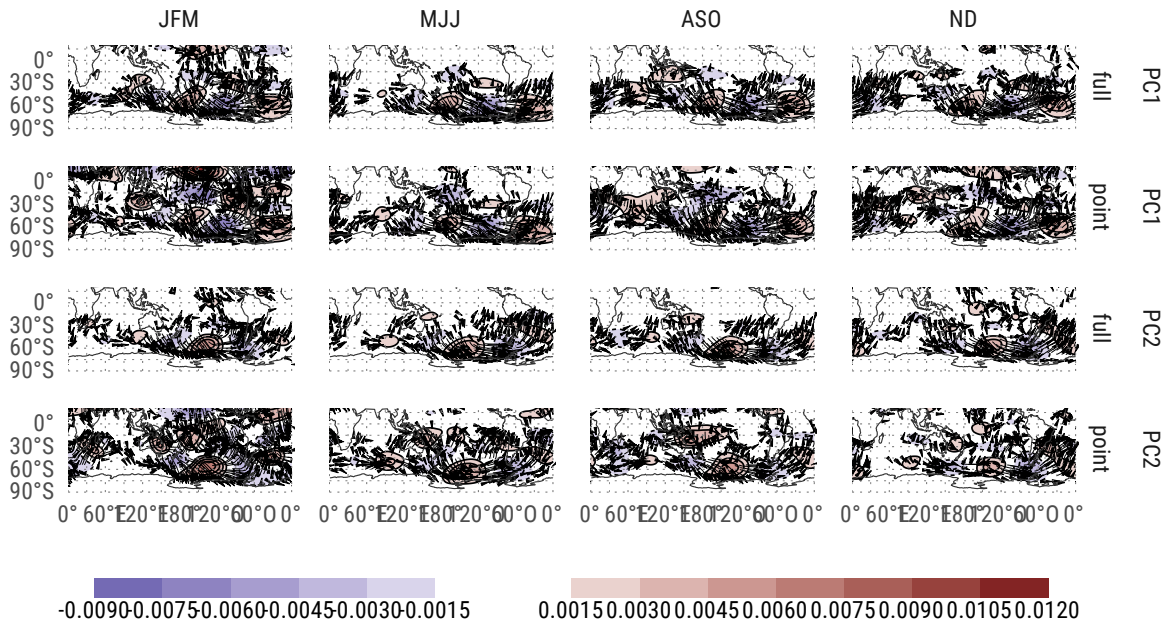


Figure 15: Zonal anomaly of regression between PCs and Psi.

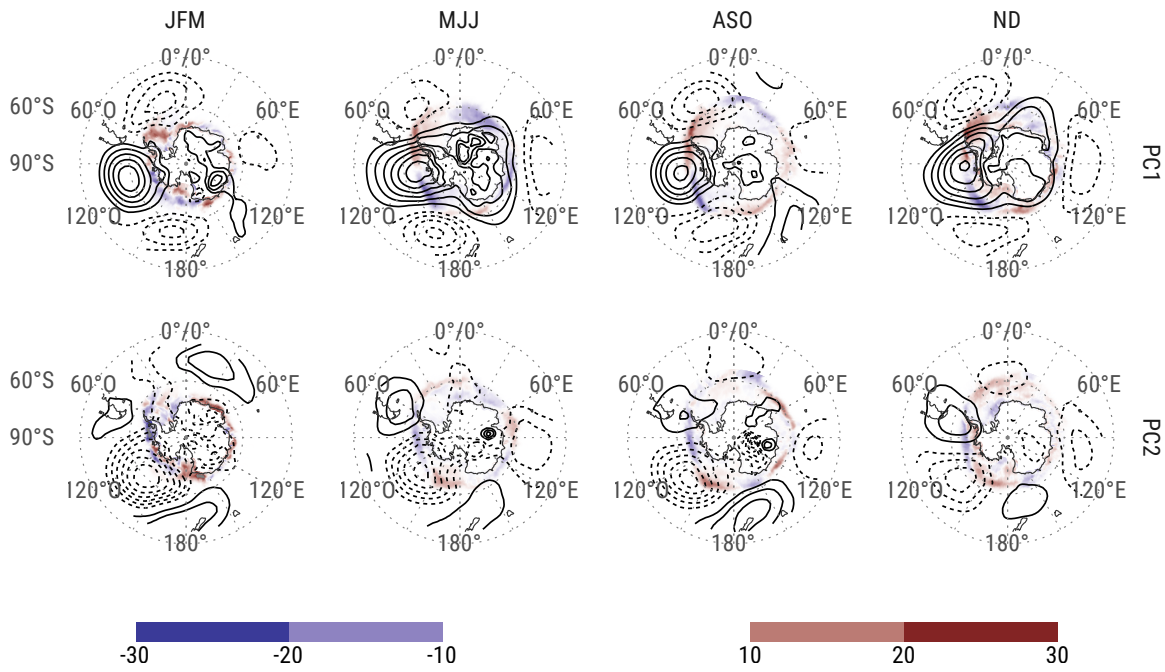


Figure 16: Regression of standarized PC with antarctic sea ice concentrations (shaded) and regression of standarized PC with 200hPa geopotential height (contours).

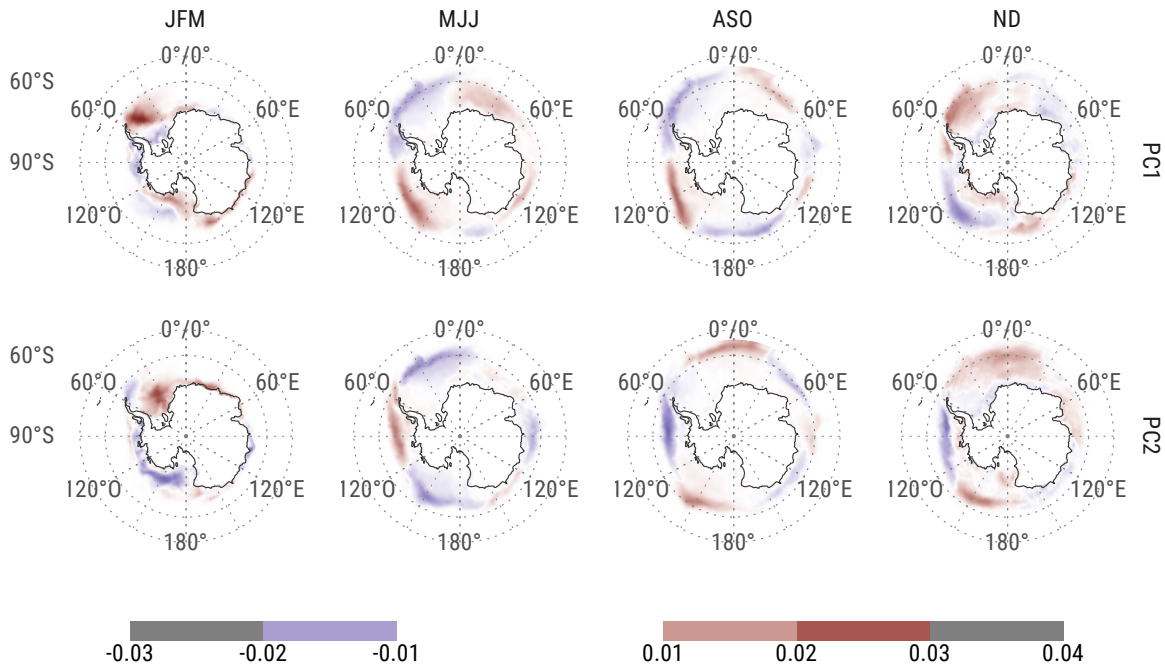


Figure 17: First 2 EOFs of antarctic sea ice concentration for each season (shaded) and regression of standarized PC (of geopotential) with 200hPa geopotential height (contours)

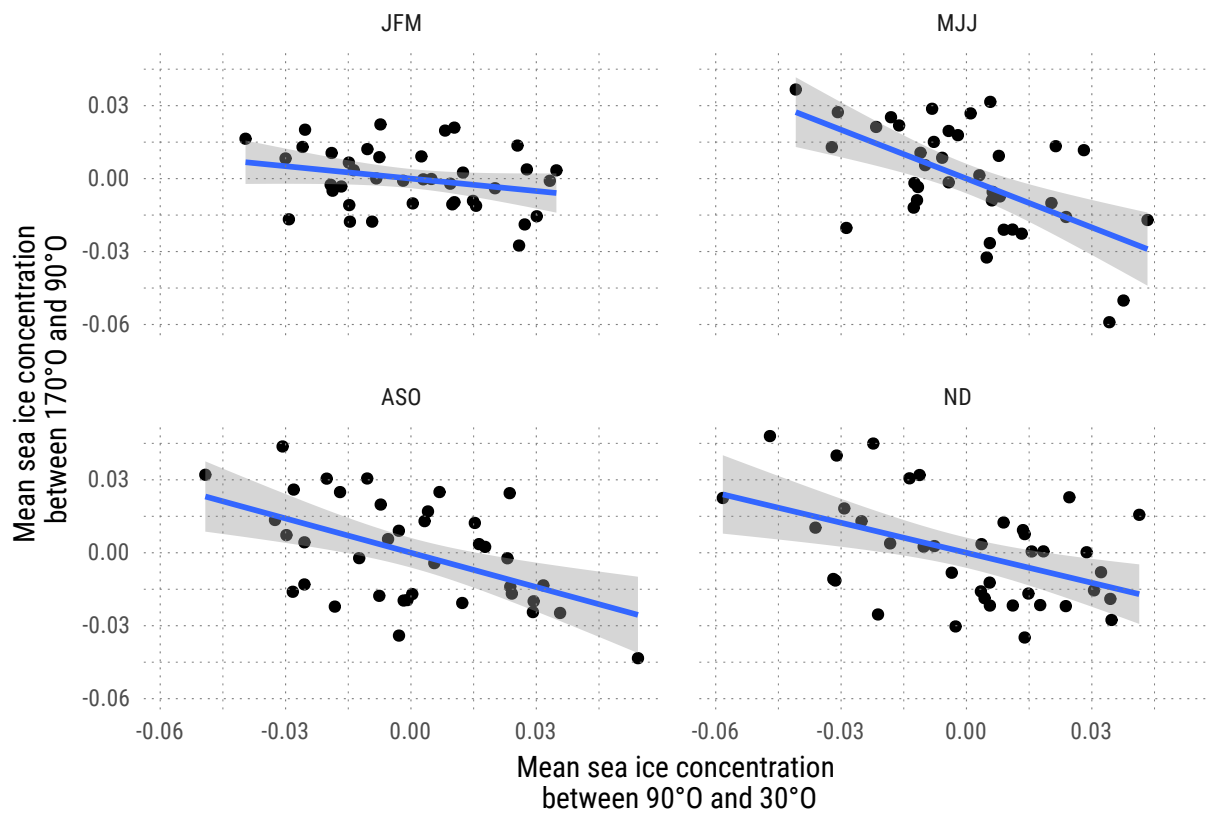


Figure 18: Mean sea ice concentration at the east of  $90^{\circ}\text{W}$  vs. at the west.

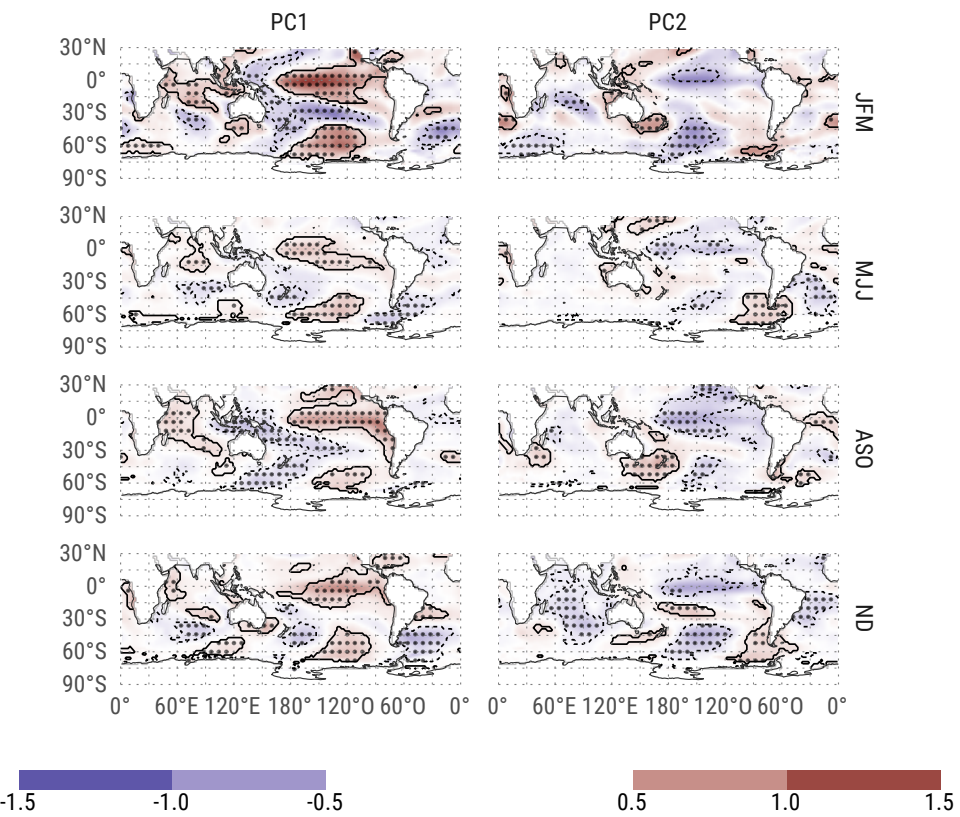


Figure 19: Regression of standarized PC with SST.

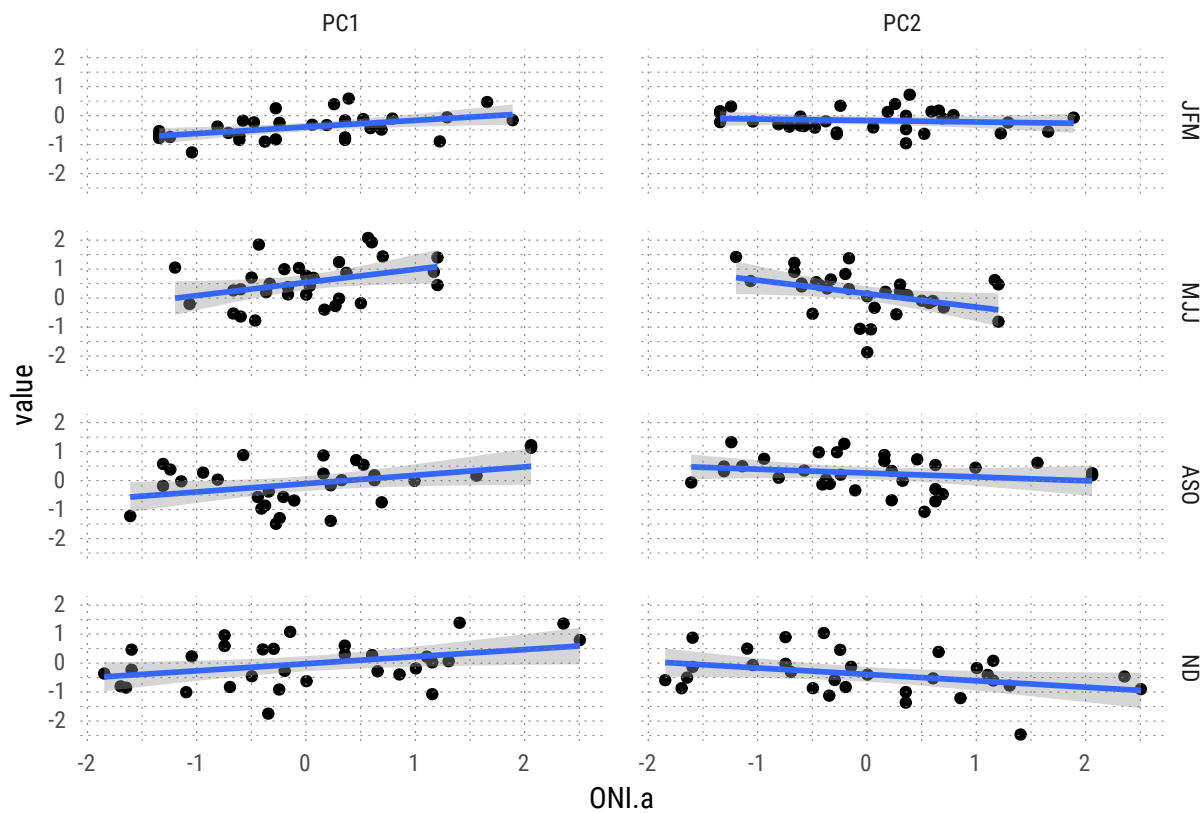


Figure 20: Relationship between PC1 and PC2 with ONI anomalies.

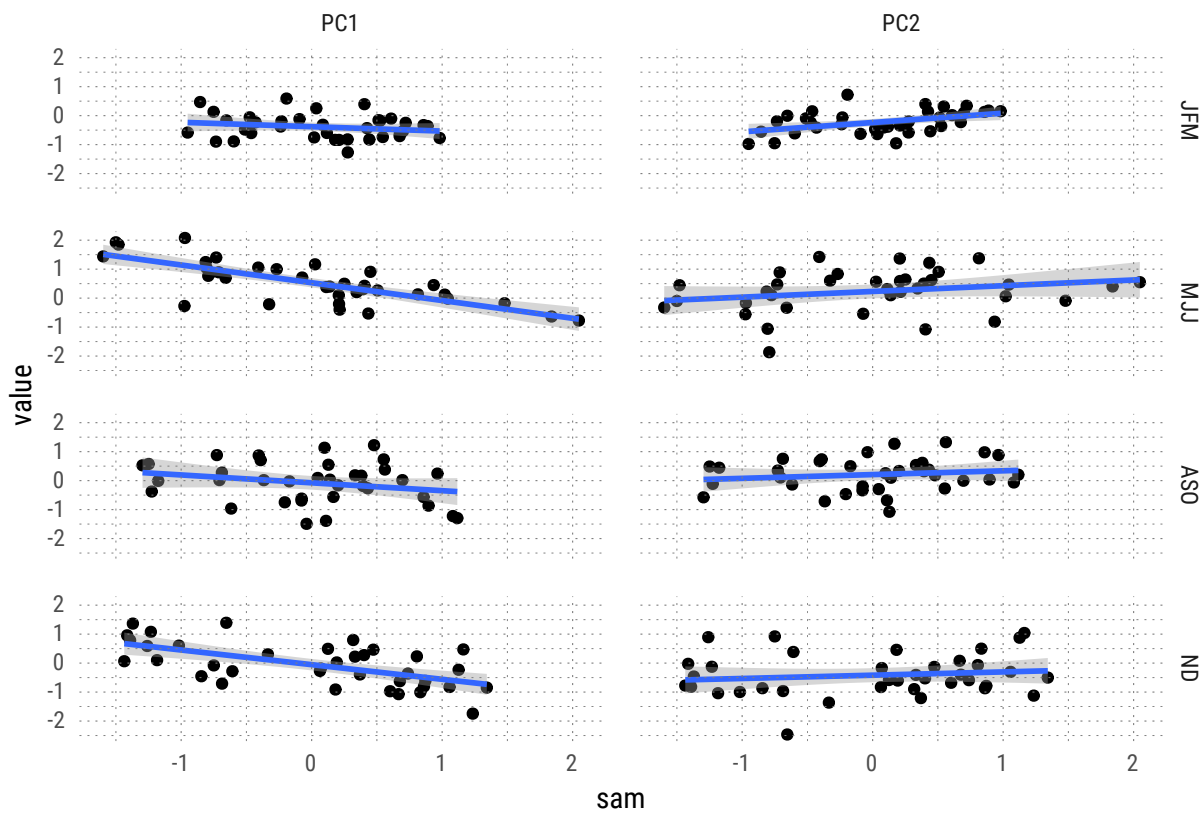


Figure 21: Relationship between PC1 and PC2 and SAM.

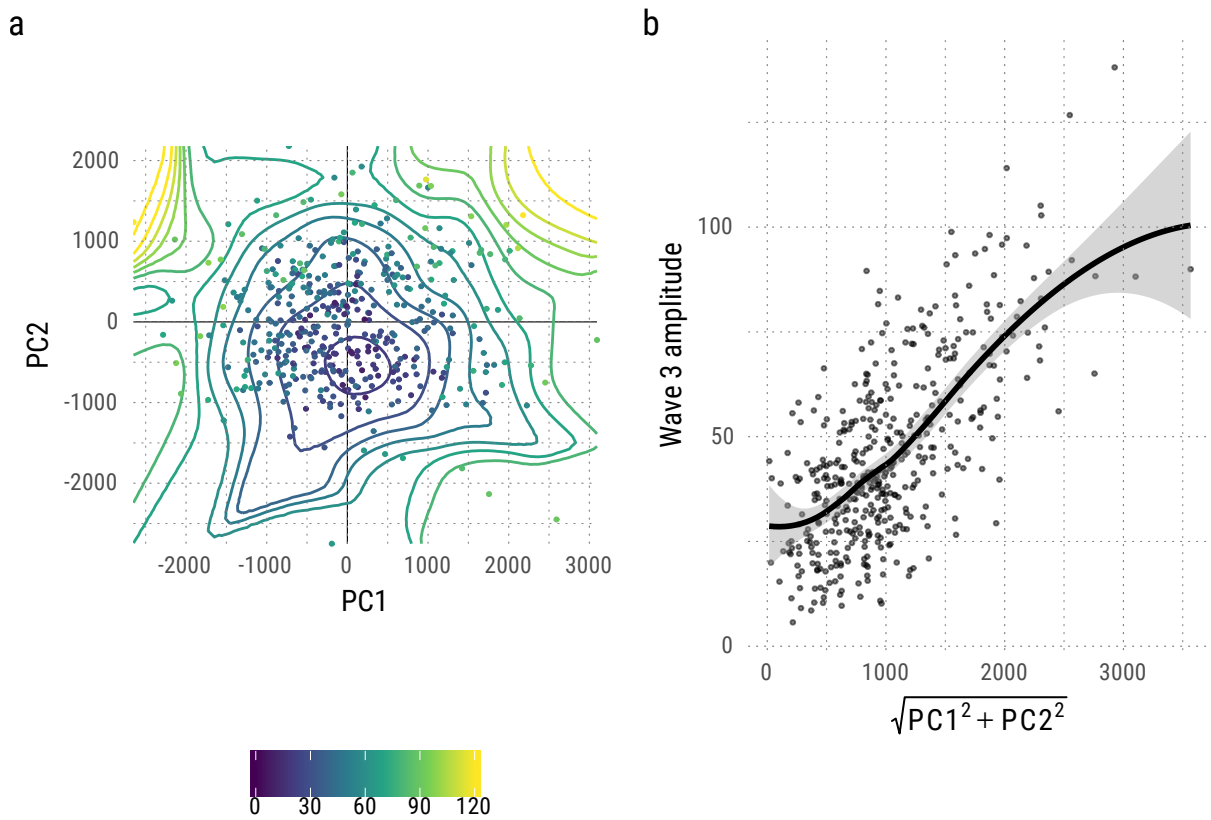


Figure 22: Relationship between 2 first EOFs and amplitude of wave 3. a) Monthly mean wave 3 amplitude as a function of PC1 and PC2; contours are a representation of the linear fit on the right. b) Amplitude of monthly mean wave 3 amplitude as a function of PC1 and PC2 magnitude.

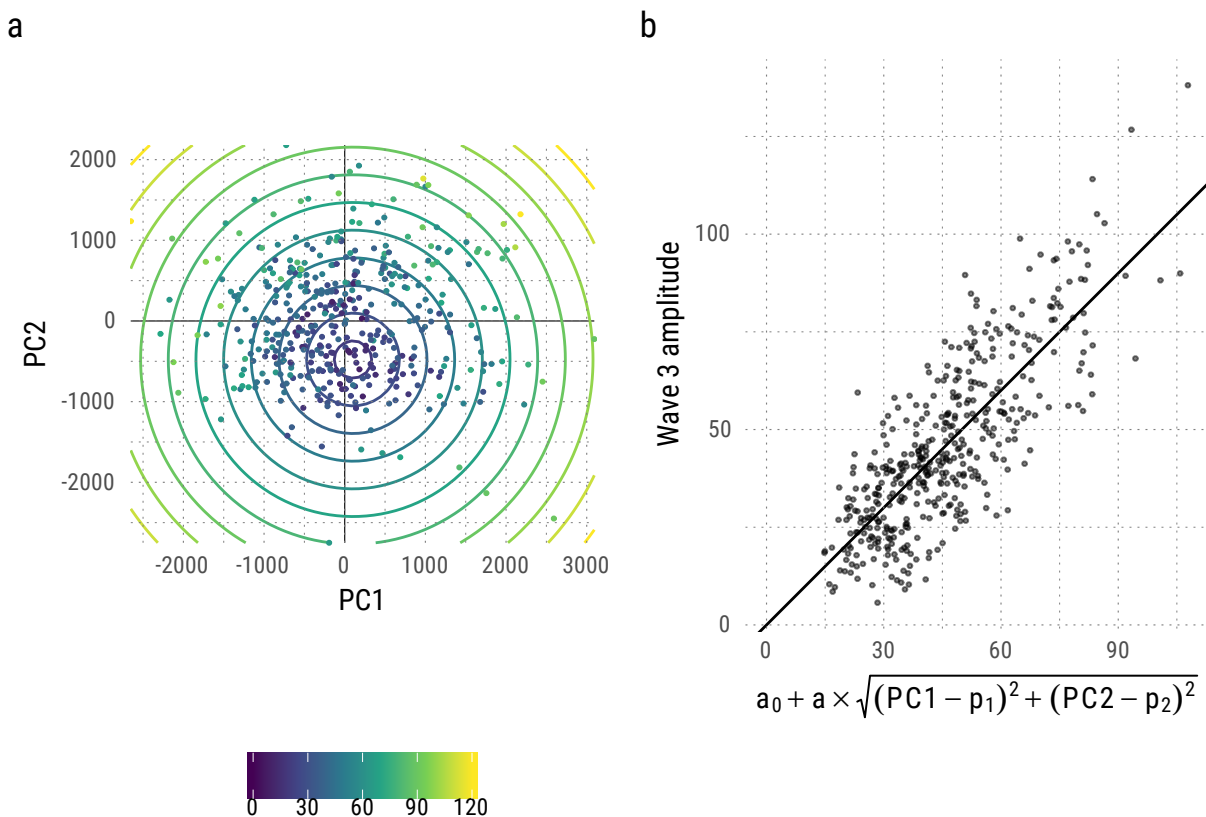


Figure 23: algo

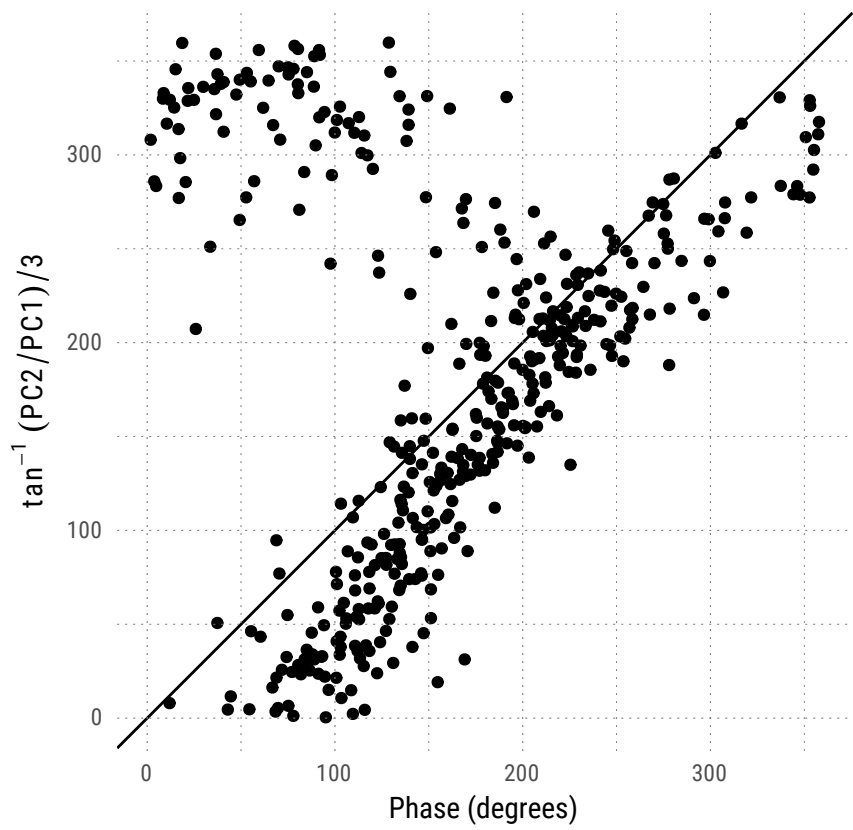


Figure 24: otra cosa

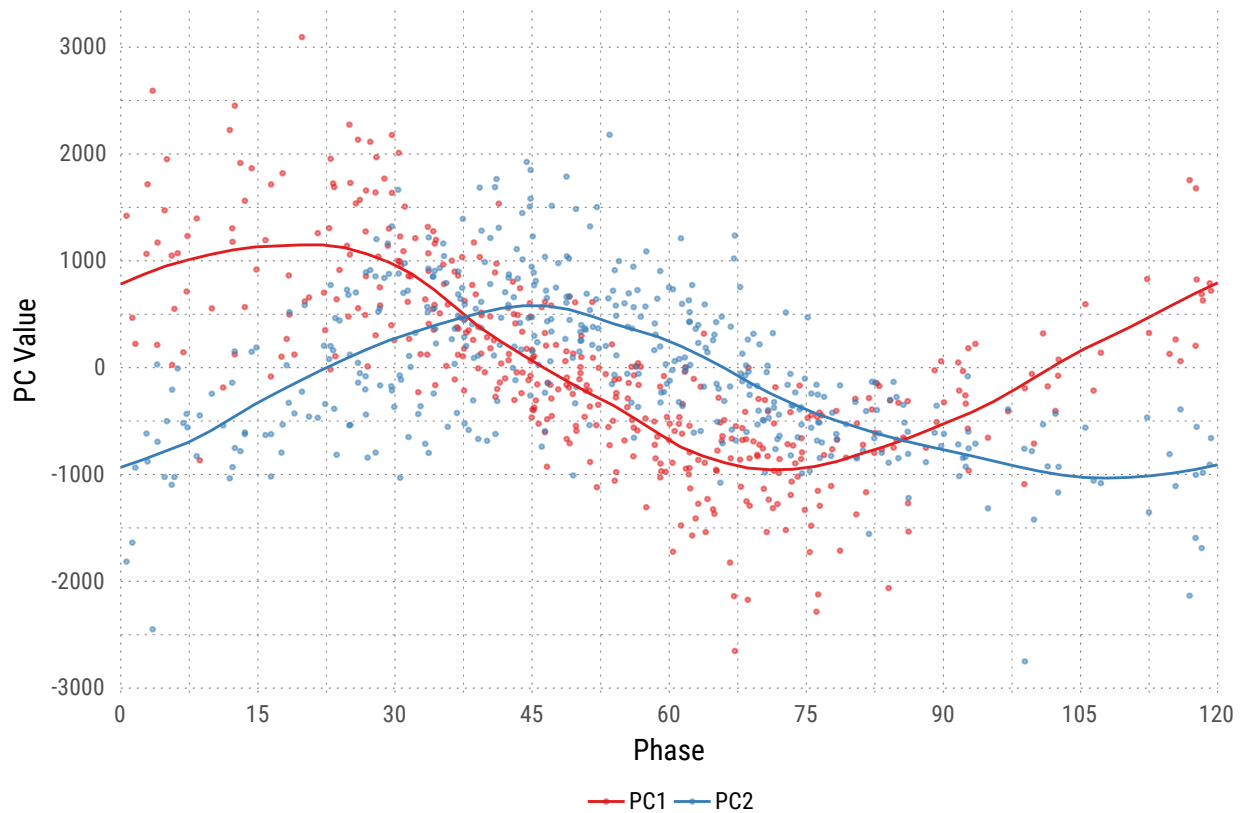


Figure 25: Phase of zonal wave 3 and value of PCs 1 to 2. The line is a loess smooth.

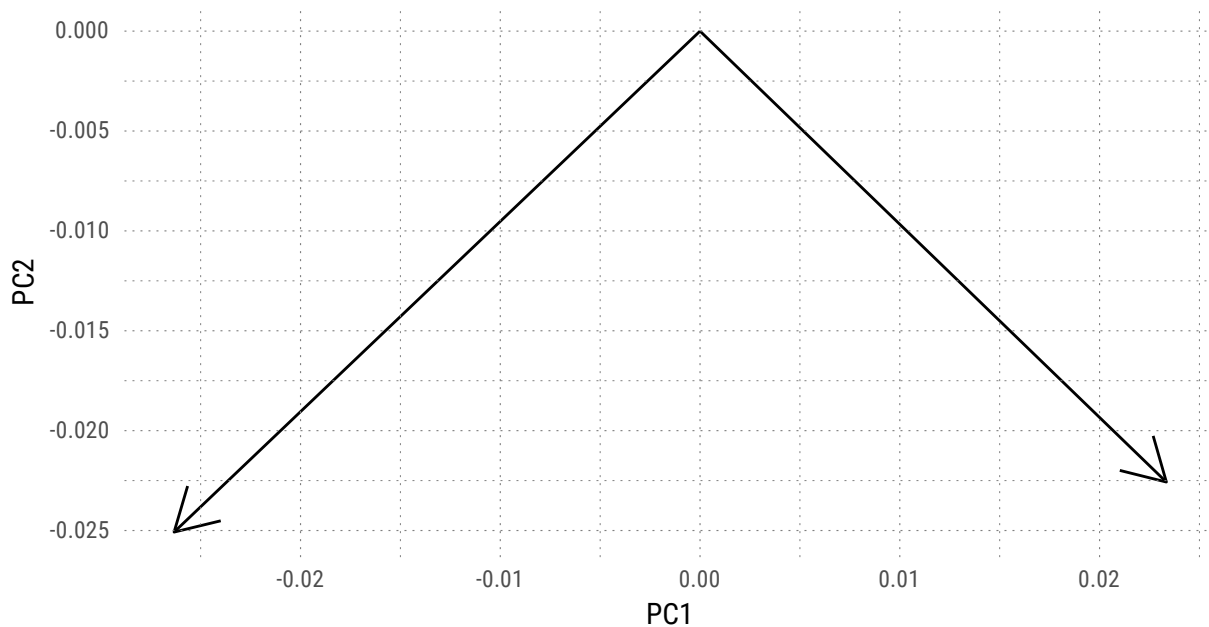


Figure 26: ultima cosa